MICROMECHANICAL RESONANT MAGNETIC SENSOR IN STANDARD CMOS

Beverley Eyre* and Kristofer S. J. Pister**
*University of California at Los Angeles
Los Angeles, CA 90024, USA, eyre@icsl.ucla.edu
**University of California at Berkeley
Berkeley, CA 94720, USA pister@eecs.berkeley.edu

SUMMARY

A novel magnetic field sensor has been fabricated using xenon difluoride etching of standard CMOS . The field is detected by measuring the vibration amplitude of a mechanical Lorentz force oscillator. The oscillator consists of a current loop on a silicon dioxide plate. Amplitude is detected with a polysilicon piezoresistor Wheatstone bridge. The devices were made in the Orbit 2 micron N-well process through MOSIS.

Keywords: resonant sensor, magnetic sensor, CMOS magnetometer

BACKGROUND

Magnetic sensors using the Hall effect as their principle of transduction are commonly made in standard CMOS and have reached a high level of predictable performance and utility [1]. However, semiconductor magnetic sensors based in silicon have intrinsic limits to their sensitivity and resolution which may limit future gains in performance [2].

With this in mind magnetic sensors of different types are being explored with the hopes of expanding the range of applications as well as the performance of CMOS based magnetic sensors. The work described here is one such and is based on a micro electromechanical systems (MEMS) approach.

Magnetic sensors and actuators using metal loops on undercut plates have been described in previous work both in CMOS and other processes [3]-[4]. A device similar to the one described here was proposed by Kadar et al. [3] using a custom process and capacitive sensing.

DESCRIPTION

These devices were fabricated using the Orbit 2 micron N-well process through the MOSIS service. After fabrication an unmasked etch using xenon difluoride [5] is performed in order to free the mechanical system and allow it to rotate.

The sensor consists of an oxide plate held suspended over an etched cavity in the silicon substrate by two sets of support beams (fig. 1). The support beams jut from the edges the etched pit near the center of the plate's long side. At the end of these beams, and perpendicular to them, are 'L' shaped beams which travel the length of the plate's long side and connect to the suspended plate near its end.

The 'L' beams on one side of the plate contain two polysilicon piezoresistors which act as the active pair of a set of four resistors forming a Wheatstone bridge (fig. 2). This bridge transduces a change in resistance due to the strain experienced by the piezoresistors when the 'L' beams

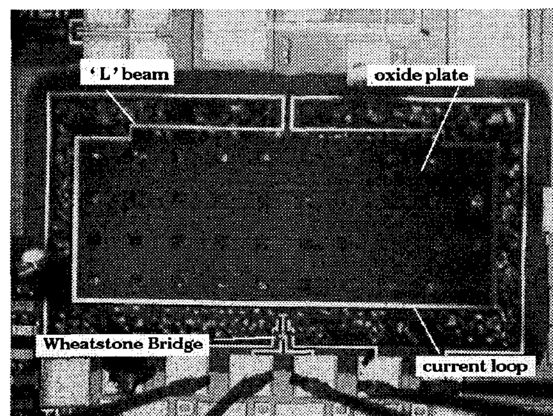

Fig. 1. Top view photomicrograph of sensor. An oxide plate is suspended over an etched cavity in silicon substrate held by torsional support beams and 'L' shaped beams. On one side of the plate is a Wheatstone bridge and on the other a current loop comes onto on off from the plate. The dark rim around the structure is the XeF_2 etch front.

bend into a change of voltage. This signal can then be sent to electronics for processing.

The set of beams on the other side of the oxide plate are used to bring a metal loop onto and off from the plate. This 'current loop' encircles the plate around its perimeter. During operation a sinusoidal signal is sent through the current loop whose function is to interact with the magnetic field and produce a force which acts on the plate.

ANALYSIS

The sensor is placed in a transverse magnetic field while a sinusoidal current is excited within the loop. This will generate a force which tends to push up on one side of the plate and down on the other (fig. 3). This force is given by:

$$F_s = I_L L_s B_x \tag{1}$$

where I_L is the loop current, B_x is the magnetic field across the plate, and L_s is the length of the side perpendicular to the magnetic field. F_s is the force on only one side of the plate.

The plate will rotate about an axis running through the support beams and create a strain in the piezoresistors. For a small rotation, the total moment experienced at the base of the bending beams will be:

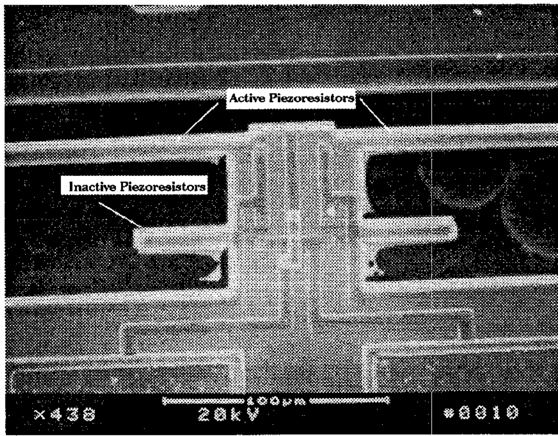

Fig. 2. Close-up of the Wheatstone bridge. The active resistors are contained within the 'L' beams and are strained when the plate rotates. The passive resistors are designed to be in close proximity to the active in order to minimize offset and temperature sensitivity.

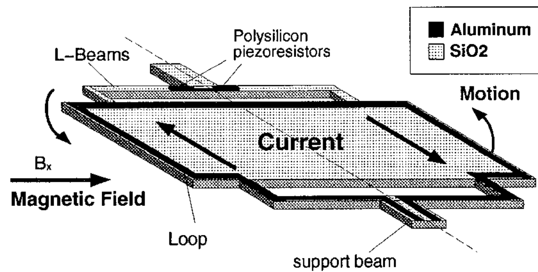

Fig. 3. Schematic showing the operation of the sensor. The current loop is excited by a sinusoidal signal while the sensor is placed in a transverse magnetic field. This will generate a torque which pushes the plate up on one side and down on the other. Because the signal is a sinusoid, the plate will rock with a see-saw motion.

$$M = 2F_s L_{ma} \tag{2}$$

where L_{ma} is the length from the end of the plate to the base of the piezoresistors. The moment is proportional to the area of the plate $A_p = 2L_s \times L_{ma}$.

The strain felt by the piezoresistors is:

$$\epsilon = \frac{Mz}{EI_b} \tag{3}$$

where z is the distance from the neutral axis of the bending beam to the polysilicon piezoresistors and EI_b is the total flexural rigidity of all four beams.

These resistors are two in a set of four configured in a Wheatstone bridge (fig. 2). The change in resistance is related to the strain by the gauge factor G, defined by:

$$\frac{\Delta R}{R} = G\epsilon \tag{4}$$

For n-type polysilicon G is roughly $\simeq -20$ [6].

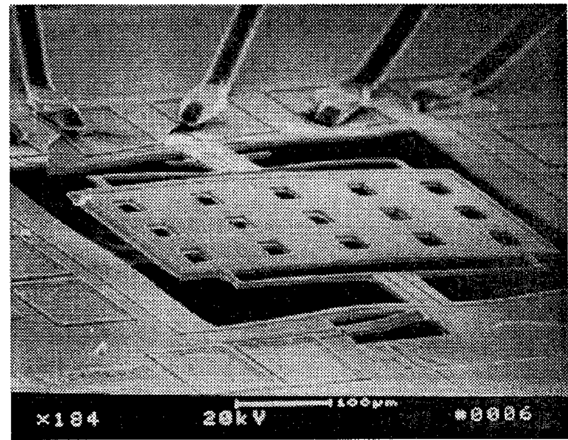

Fig. 4. SEM of a smaller version of the resonant mechanical sensor. The oxide plate is seen to have a small stess gradient. The holes on the plate are for the purpose of reducing the etch time. This device was released using 50 one minute pulses of XeF_2 gas at room temperature. The etch pressure was $\simeq 2\,Torr$.

The change in resistance of the strained piezoresistors becomes a change in voltage within the Wheatstone bridge and thus the magnetic field is transduced into a voltage. For a bridge with two active resistors:

$$\frac{\Delta V}{V} = \frac{\Delta R}{2R} \tag{5}$$

This voltage can be used as the signal input to on-chip signal processing circuits in the creation of a 'smart' sensor. This step of integration has not yet been taken with this sensor, though similar systems have been demonstrated in the same process [7].

From this last we get the expression for the sensitivity of the sensor:

$$S = \frac{\Delta V}{\Delta B} = \frac{zGI_L V A_p}{EI_b} \tag{6}$$

When running the sensor at the resonant frequency of the mechanical system the sensitivity is multiplied by the quality factor Q.

The sensitivity can be expressed as a function of four factors: 1) the Q of the sensor; 2) a constant made up of process parameters, physical constants, and the flexural rigidity of the beams; 3) The area of the plate; 4) a term with units of power made up of the Wheatstone bridge voltage multiplied by the loop current.

The resonant frequency of the system can be approximated by:

$$\omega_o = \sqrt{\frac{K}{m}} \tag{7}$$

where

$$K = \frac{Ea^3 b}{4L_b^3} \tag{8}$$

is the spring constant of four beams, m is the mass of the plate-beam system, E is the Young's Modulus of the

bending beams, L_b is the length of the bending beam, and a and b are the thickness and width of the beam, respectively.

RESULTS AND DISCUSSION

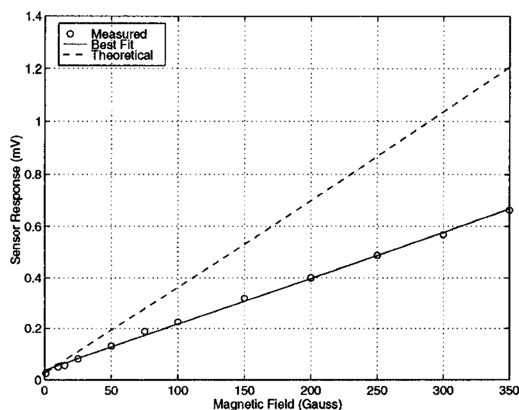

Fig. 5. Wheatstone bridge output versus transverse magnetic field. Loop current was 10mA at 2.5kHz. Bridge excitation was 1V. The output voltage plotted here is the amplitude of the output sinewave.

Testing was performed by independently varying conditions of magnetic field strength, loop current and Wheatstone bridge voltage. Figure 5 plots the voltage output of the Wheatstone bridge as a function of magnetic field strength. There is an AC loop current of 10 milliamps running at 2.5kHz, the mechanical resonant frequency of the plate-beam system, and a 1 volt drop across the Wheatstone bridge. These values were chosen not to test the ultimate sensitivity of each device, but merely to compare the measured response to the theoretical model. For this reason they are small and well within the safe operating range of the devices.

The response is linear with a slight voltage offset. This offset corresponds to roughly fifteen Gauss.

Frequency measurements for two generations of devices was performed. The first generation device had 'L' beams 8 μm wide and during the etching process tended to crack. This exposed the polysilicon resistors to the XeF_2 and resulted in many of the active resistors being etched. In the second generation the beams were widened to 10 μm and this problem was not seen.

Figures 7 and 6 show the Bode plots of the two generations of devices. While the DC level of the first generation seems closer to the theoretical model, the resonant frequency of the second generation is the more accurate. The smaller Q in the later generation may be due to wider metal lines in the 'L' beams, creating more internal damping within the beams themselves.

The best fit curves in Figures 7 and 6 are two pole and four pole Bode plots with the resonant frequency, DC response, and damping factors as input parameters. The theoretical curve is calculated from equations (6) and (7) and from the magnetic field, voltages, and currents used in the experiment. The damping factor used in this calculation was the one measured during testing.

Figure 8 shows the frequency response of the system with no applied magnetic field. Here the output voltage of the Wheatstone bridge is due to changing temperature in the

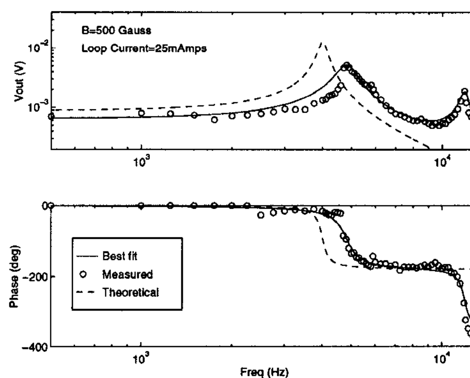

Fig. 6. Bode plot of first generation device. This device shows a resonant peak near the predicted value, and an additional peak at roughly twice that value. The Q of this device is $\simeq$ 10 at the first resonant frequency. Testing at low pressure indicates that the damping is probably internal and due to the aluminum traces that travel onto and off the plate via the 'L' beams.

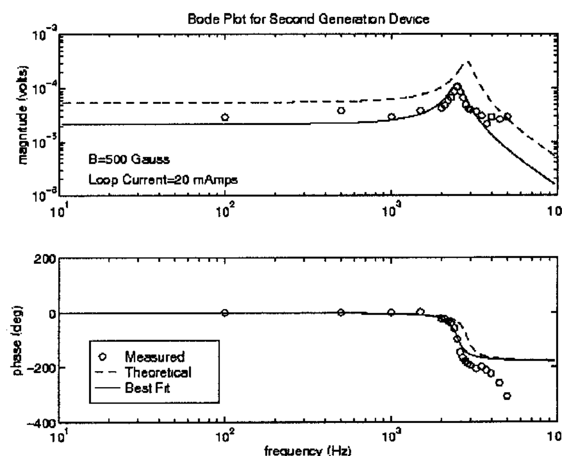

Fig. 7. Bode plot of second generation device. This version of the sensor had wider 'L' beams than the first generation. This widening of the beams may account for the slight decrease in Q.

sensor, a consequence of the loop power: $I_{loop}^2 \times R_{loop}$, where R_{loop} is the resistance of the loop metalization, around 50 ohms. In this experiment the peak loop power was slightly over 4.5 mWatts.

In this test one piezoresistor from the L beams was connected to three off-chip resistors to form a Wheatstone bridge and a current of 9.5 mA was sent through the loop at a series of frequencies. The voltage across the bridge was 2 volts. The bridge output had a DC component and an AC component with frequency twice the loop current frequency, as expected from I_{loop}^2. The DC component stayed constant over all loop current frequencies. The AC component had constant amplitude up to roughly 10 Hz, then began to decay as the loop current frequency increased. This indicates that at the resonant frequencies of these magnetometers the thermal excitation of the piezoresistors will be small but measurable. Fortunately, the thermal re-

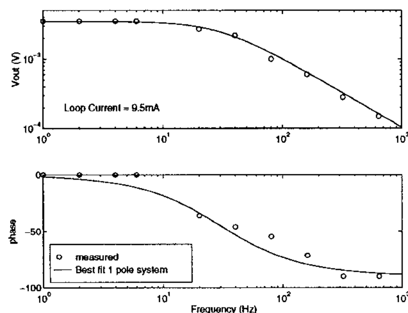

Fig. 8. Thermal response of a Wheatstone bridge versus frequency of the loop current. 4.5 mW peak power in the loop. No applied magnetic field. The bridge has a single on-chip and three off-chip resistors.

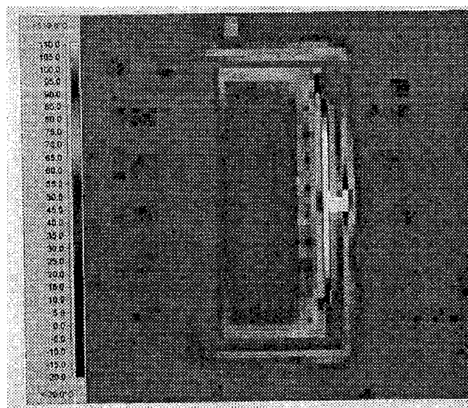

Fig. 9. Thermal image of sensor operating at 2Hz. At low frequency the plate has enough time to reach a temperature of over 100^oC*. This 'hot spot' is located at the support and 'L' beams where the current comes onto the plate. On the opposite side where the Wheatstone bridge is located the temperature is as cool as the surrounding substrate. Operated at the resonant frequency the hot spot temperature drops by over* 40^oC*.*

sponse frequency is at twice the signal frequency, and the use of co-located bridge resistors attenuates this thermal response still further.

Figure 9 is a thermal image of the sensor operating at 2Hz. It is seen that the highest temperature is at the support beam where the current loop comes onto the plate. The Wheatstone ridge is on the other side of the plate and is relatively cool.

Testing was performed to find the relation between Q and pressure. The results indicated that there was another source of damping in addition to viscous damping. This additional damping could be due to the aluminum traces that bring the current onto the loop and are within the 'L' beams. This damping is dominant and consequently the Q increased only slightly in low pressure.

CONCLUSION

A micromechanical resonant magnetic field sensor has been fabricated in a standard commercial CMOS process with a simple, maskless, post-CMOS etching. Several of these sensors have been tested and display sensitivities of hundreds of millivolts per Tesla. Resonant frequencies in the kiloHertz range with quality factors of roughly 10 are typical for devices taking roughly $0.5\,mm^2$ of die area.

The quality factor of the oscillator affects sensitivity directly. Vacuum testing of these devices indicates that the low Q is not due to viscous damping, but is primarily due to structural damping. There is some evidence to support the idea that this damping is due to the aluminum traces in the beams providing the loop current. Other factors include the non-ideal boundary conditions resulting from the xenon difluoride release etch, and the non-ideal and poorly characterized multilayer dielectric films which make up the structure of the device.

Assuming thermal noise in the piezoresistors as the ultimate limitation of resolution for this sensor, this second generation device should be capable of measuring signals as small as 25 $\mathrm{nTesla}/\sqrt{\mathrm{Hz}}$. With future design improvements 1-10 $\mathrm{nTesla}/\sqrt{\mathrm{Hz}}$ should be possible.

ACKNOWLEDGMENTS

Thank to Russell Lawton and Ronald Ruiz in the MEMS Reliability Section at the Jet Propulsion Laboratory for their help with thermal imaging. This work was supported by NSF under IRI-9321718 and DARPA.

REFERENCES

[1] H. Baltes and R. Popovic. Integrated semiconductor magnetic field sensors. *Proc. IEEE*, 74(8):1107–1132, August 1986.

[2] A. Chovet, C. Roumenin, G. Dimopoulos, and N. Mathieu. Comparison of noise properties of different magnetic-field semiconductor integrated sensors. *Sensors and Actuators*, A22(1-3):790–4, March 1990.

[3] Z. Kadar, A. Bossche, and J. Mookinger. Integrated resonant magnetic-field sensor. *Sensors and Actuators*, A41(1-3):66–69, April 1994.

[4] B. Shen and W. Allegretto. CMOS micromachined cantilever-in-cantilever devices with magnetic actuation. *IEEE Electron Device Letters*, 17(7):372–374, July 1996.

[5] F. Chang, R. Yeh, G. Lin, P.B. Chu, E. Hoffman, E. Kruglick, and K. Pister. Gas-phase silicon micromachining with xenon difluoride. *SPIE Symposium on Micro-machining and Micro-fabrication*, 2641:117–128, Austin, TX, October 1995.

[6] P.J. French and A.G.R. Evans. Polycrystalline silicon strain sensors. *Sensors and Actuators*, 8(3):219–225, November 1985.

[7] G. Lin, K.S.J Pister, and K.P. Roos. Standard CMOS piezoresistive sensor to quantify heart cell contractile forces. *Proc. IEEE, MEMS-96 Workshop on Micro Electro Mechanical Systems*, pages 150–155, San Diego, Feb 1996.